

YOUNG STARS IN AN OLD BULGE: A NATURAL OUTCOME OF INTERNAL EVOLUTION IN THE MILKY WAY

M. NESS¹, VICTOR P. DEBATTISTA², T. BENSBY³, S. FELTZING³, R. ROŠKAR⁴,
D. R. COLE², J. A. JOHNSON^{5,6}, AND K. FREEMAN⁷

¹ Max-Planck-Institut für Astronomie, Königstuhl 17, D-69117 Heidelberg, Germany; ness@mpia.de

² Jeremiah Horrocks Institute, University of Central Lancashire, Preston PR1 2HE, UK

³ Lund Observatory, Department of Astronomy and Theoretical Physics, Box 43, SE-221 00 Lund, Sweden

⁴ Institute for Theoretical Physics, University of Zürich, Winterthurerstrasse 190, Zürich CH-8057, Switzerland

⁵ Department of Astronomy, Ohio State University, 140 W. 18th Avenue, Columbus, OH 43210, USA

⁶ Center for Cosmology and Astro-Particle Physics, Ohio State University, 191 West Woodruff Avenue, Columbus, OH 43210, USA

⁷ Research School of Astronomy and Astrophysics, Mount Stromlo Observatory, Cotter Road, Weston Creek, ACT 2611, Australia

Received 2013 December 22; accepted 2014 April 11; published 2014 May 12

ABSTRACT

The center of our disk galaxy, the Milky Way, is dominated by a boxy/peanut-shaped bulge. Numerous studies of the bulge based on stellar photometry have concluded that the bulge stars are exclusively old. The perceived lack of young stars in the bulge strongly constrains its likely formation scenarios, providing evidence that the bulge is a unique population that formed early and separately from the disk. However, recent studies of individual bulge stars using the microlensing technique have reported that they span a range of ages, emphasizing that the bulge may not be a monolithic structure. In this Letter we demonstrate that the presence of young stars that are located predominantly nearer to the plane is expected for a bulge that has formed from the disk via dynamical instabilities. Using an N -body + smoothed particle hydrodynamics simulation of a disk galaxy forming out of gas cooling inside a dark matter halo and forming stars, we find a qualitative agreement between our model and the observations of younger metal-rich stars in the bulge. We are also able to partially resolve the apparent contradiction in the literature between results that argue for a purely old bulge population and those that show a population comprised of a range in ages; *the key is where to look*.

Key words: Galaxy: bulge – Galaxy: evolution – Galaxy: formation – Galaxy: stellar content

Online-only material: color figures

1. INTRODUCTION

The boxy/peanut-shaped bulge of the Milky Way was revealed in the star counts from the Two Micron All Sky Survey (López-Corredoira et al. 2005) and more recently has been mapped in detail across the inner extent using red clump stars (Wegg & Gerhard 2013). It has been proposed that small boxy or peanut-shaped bulges form via internal evolution of the disk (Combes & Sanders 1981). As the disk becomes unstable, it forms a rotating bar which buckles and heats the disk vertically (Raha et al. 1991). The orbits of the stars originally in the bar are extended vertically into orbits which now define the boxy/triaxial/peanut-shaped bulge. A number of properties of the bulge of the Milky Way have recently been shown to be consistent with the generic properties of N -body models that form a bulge via internal evolution from the redistributed stars of the disk. These include the kinematics of stars in the bulge (Howard et al. 2008; Kunder et al. 2012; Ness et al. 2013b) and the X-shaped profile (McWilliam & Zoccali 2010; Nataf et al. 2010), which provide important observational constraints on models of formation (Shen et al. 2010; Ness et al. 2012; Li & Shen 2012; Gardner et al. 2014). Another important observational constraint on the formation of the bulge is stellar ages.

Studies of the color–magnitude diagrams of several fields in the bulge have shown that the best isochrone fits support a purely old (>10 Gyr) stellar population (e.g., Ortolani et al. 1995; Zoccali et al. 2003; Sahu et al. 2006; Clarkson et al. 2008; Brown et al. 2010; Valenti et al. 2013). This has been interpreted as evidence for a classical bulge population, formed rapidly at early times and before the disk, via mergers or dissipational

collapse processes (Ortolani et al. 1995; Zoccali et al. 2003). Recent studies interpret different signatures of formation in the boxy/peanut morphology and the stellar ages and metallicities to argue for a composite bulge. These studies (e.g., Babusiaux et al. 2010; Hill et al. 2011) conclude that dissipational collapse formation has played an important role in the formation of the bulge, in addition to the dynamical instability processes. Disk galaxies with no bulges or with relatively small boxy or peanut-shaped bulges like the Milky Way are quite common (Lütticke et al. 2004) and their formation route in the context of the evolution of the universe is critical for our understanding of galaxy formation (e.g., Barentine & Kormendy 2012). To constrain the formation processes of the Milky Way and interpret the signatures of formation, including ages, comparisons to models of individual galaxies are key.

2. AGES OF INDIVIDUAL BULGE STARS

The old stellar ages reported from the photometric studies seem at odds with the studies that exploit microlensing events of the dwarf and subgiant bulge stars, which uniquely allow ages of individual bulge stars to be determined. The microlensing studies have demonstrated that the more metal-rich stars in the bulge ($[\text{Fe}/\text{H}] > -0.4$ dex) show a range in stellar ages from 3–12 Gyr, as shown in Figure 1 (Bensby et al. 2011, 2013). This figure also shows our simulation’s stellar distribution in $[\text{Fe}/\text{H}]$ –age space. These younger stars are not expected to be present for a classical bulge population, formed rapidly at early times and before the disk, via dissipational or merger processes. If the bulge formed via internal disk instabilities rather than

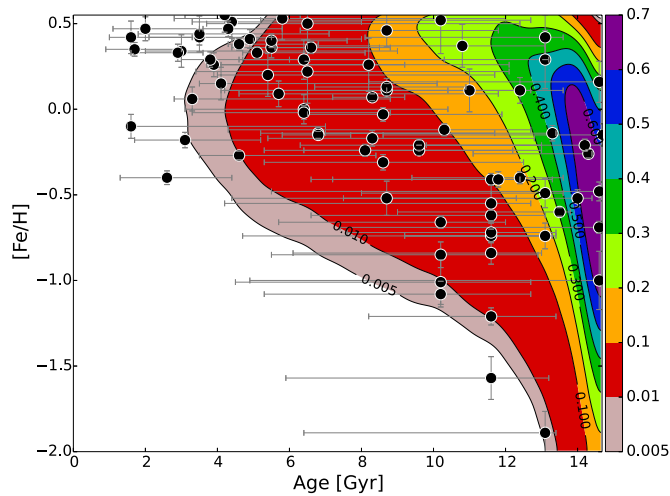


Figure 1. Age–metallicity diagram of the 58 microlensed bulge dwarfs (Bensby et al. 2013) and an extra 22 dwarfs observed to date as part of their ongoing target of opportunity program. Note the metal-rich stars show a distribution in ages and metal-poor stars are all old. The 22 new observations will be published in T. Bensby et al. (2014, in preparation). The color map is the age–[Fe/H] density distribution of stars in the simulation over the (l, b) range of the observations. (A color version of this figure is available in the online journal.)

mergers, however, younger stars should be present due to ongoing star formation in the plane.

In this Letter, we compare the age distribution of the microlensed dwarf stars, which show a range of ages, to a high mass resolution simulation that includes star formation, as described in Section 3. We examine the stellar age distribution of the model as a function of height from the plane and [Fe/H] in Section 4 and test the apparent contradiction that exists between the range of ages reported from the microlensing studies and the old population suggested by the photometric studies.

3. THE GALACTIC MODEL

Interpreting the observational data requires models that include star formation. Until now, such predictions have come from semi-analytic models or from cosmological simulations which generally do not yet reach a resolution to resolve boxy/peanut-shaped structures. Here we use a self-consistent dissipational collapse simulation that is a higher mass resolution version of previous models (Roškar et al. 2008), with 10^7 stars and a spatial resolution of 50 pc. In this model, a hot gas corona in a Navarro–Frenk–White (Navarro et al. 1997) dark matter halo cools under self-gravity and forms a disk galaxy with a small, weakly triaxial bulge. The evolution of this model in isolation thus reflects internal processes only as there are no interacting companions during the evolution. The model was presented in Gardner et al. (2014) and the evolution of its nucleus will be presented in D. R. Cole et al. 2014 (in preparation). For this Letter the model is studied after evolving for 10 Gyr. We emphasize that this model was not designed to match the Milky Way and our analysis is qualitative. However, we find a remarkable qualitative agreement with a number of observational signatures. We have scaled the model (by a factor of 1.2) to match the bar size to that of the Milky Way of about 3.5 kpc (Robin et al. 2012) and placed the bulge at 8 kpc away from the Sun, at an angle of 27° with respect to the line of sight (Wegg & Gerhard 2013). The model is shown in Figure 2 with the Sun placed at $y = -8$ kpc. It qualitatively reproduces the observed kinematic profile that is generic to models of bulges formed via internal evolution of

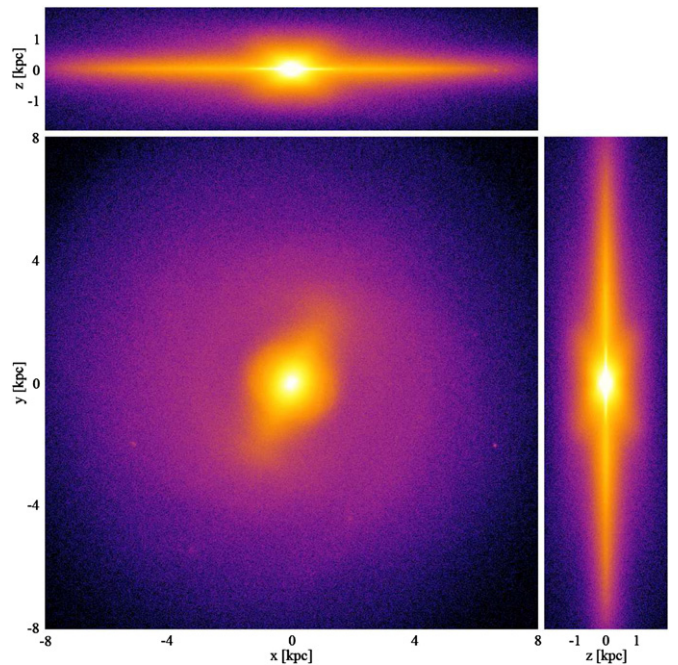


Figure 2. Mass surface density of the model projected onto the x – y , x – z , and y – z planes as indicated. Note the boxy shape and X-structure in the y – z projection at right.

(A color version of this figure is available in the online journal.)

the disk (Shen et al. 2010; Ness et al. 2013b) as well as the X-shaped profile that is seen in the Milky Way (Gardner et al. 2014).

4. COMPARISON TO OBSERVATIONAL DATA

The resolution of our model is much higher than in previous models, and includes gas and stellar chemistries not previously employed in such studies, so this is the first time structure can be studied in such detail. We wish to investigate the distribution of stellar ages in the model at different heights from the plane and at different metallicities to understand if there are young stars in the bulge and, if so, where they are concentrated. A direct comparison of the age–[Fe/H] distribution of individual stars shown in Figure 1 with the simulation requires defining the selection function of the microlensed dwarf stars, which is quite uncertain. Bensby et al. (2013) conclude that they oversample the metal-rich stars by about 50%. However, the comparison of the line-of-sight density distribution of the simulation with no selection function implemented, with the observations in Figure 1, already shows that the general trend in the age–[Fe/H] space of the observations is broadly matched by the simulation. There is a wide range of ages at high metallicities and the age range narrows sharply at lower metallicities. For this comparison, stars are taken from the model across the (l, b) range of the observations and within the inner 3 kpc. To show these distributions in the same figure, the simulation is scaled in age (to the oldest stars in the observational data of 14.7 Gyr) and in metallicity (to set the mean metallicity of the thin disk at the Sun to [Fe/H] = -0.25 ; Gilmore et al. 1995). The simulation shows a narrower age range compared to the observations. The relative density is different between model and observations, with a far lower density of young metal-rich stars compared to the microlensed dwarfs, but these details are sensitive to the selection function.

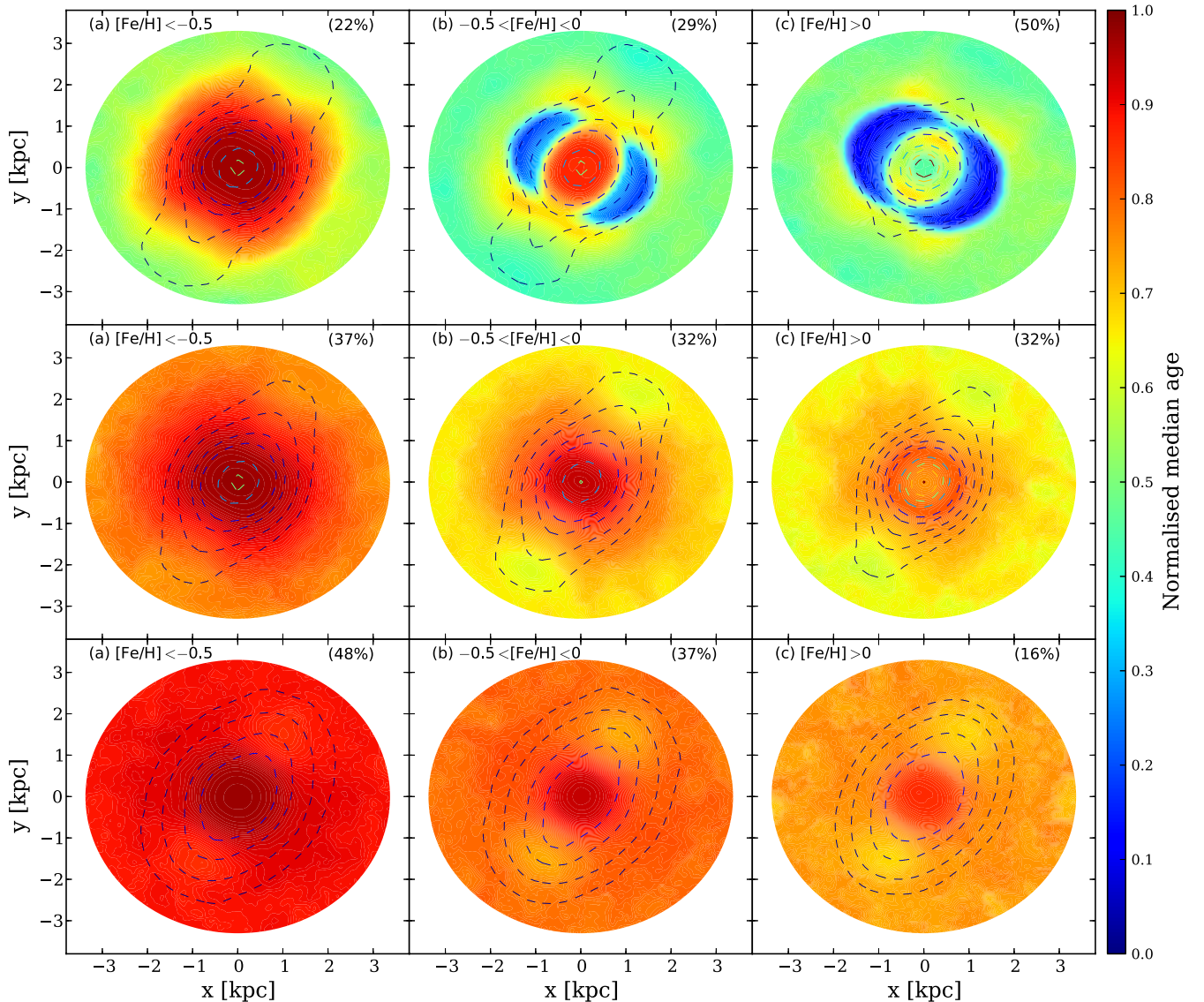


Figure 3. Median age of stars in the inner $R < 3$ kpc of the simulation showing three slices in height, $|z|$, from the plane, from top to bottom of $|z| < 0.14$ kpc, $0.14 \text{ kpc} < |z| < 0.42$ kpc, and $0.42 \text{ kpc} < |z| < 0.85$ kpc. The color scale is the normalized median age. The sub-panels represent stars of different metallicity bins: (a) $[\text{Fe}/\text{H}] < -0.5$, (b) $-0.5 < [\text{Fe}/\text{H}] < 0$, (c) $[\text{Fe}/\text{H}] > 0$. The density contours are shown to indicate the distribution of the stars in each bin. The percentage of stars in each metallicity bin is indicated in each sub-panel.

(A color version of this figure is available in the online journal.)

In order to understand the qualitative distribution of ages, we now examine different slices in height across the inner region of the simulation.

Figures 3 and 4 show the median age and age dispersion for the face-on projections of the simulation out to a radius of $R < 3$ kpc, at three slices in height, $|z|$, from the plane. An age scale normalized to the current age ($=10$ Gyr) of the simulation is used. The surface density contours illustrate the extent of the bar. These $|z|$ -slices intersect the center of the bulge at latitudes of $|b| < 1^\circ$, $1^\circ < |b| < 3^\circ$, and $3^\circ < |b| < 6^\circ$ from the plane at the center of the bulge. At each height different metallicity ranges are shown in the three sub-panels of (a) $[\text{Fe}/\text{H}] < -0.5$, (b) $-0.5 < [\text{Fe}/\text{H}] < 0$, and (c) $[\text{Fe}/\text{H}] > 0$.

4.1. The Age Distribution of Stars Across Latitude

Looking at Figure 3, it is clear that according to the model (1) the young stars are strongly concentrated very close to the

plane, (2) there is a sharp transition between young and old stars in the bulge with latitude and distinct transitions in the age distribution with longitude, and (3) the oldest stars become more centrally concentrated at larger heights from the plane. The model predicts that a few degrees can make the difference between observing a predominantly old population of stars or a population with a range of stellar ages in the inner galaxy due to these steep gradients in the age distribution in the bulge/bar and surrounding disk. Nearest to the plane around the inner region, the stars will have the largest age range, so both young and old stars will be present. The regions around the center of the bulge and ends of the bar show the most homogeneously young population. In this simulation the youngest stars are located along the edges of the bar in a thin nuclear disk which is not present at earlier times. The youngest stars in the nuclear disk in the plane (ages < 3 Gyr) are not what we compare to the microlensed dwarf observations and we have tested our model at earlier times before this disk formed and verify that similar to this snapshot, there are young stars heated from the disk to

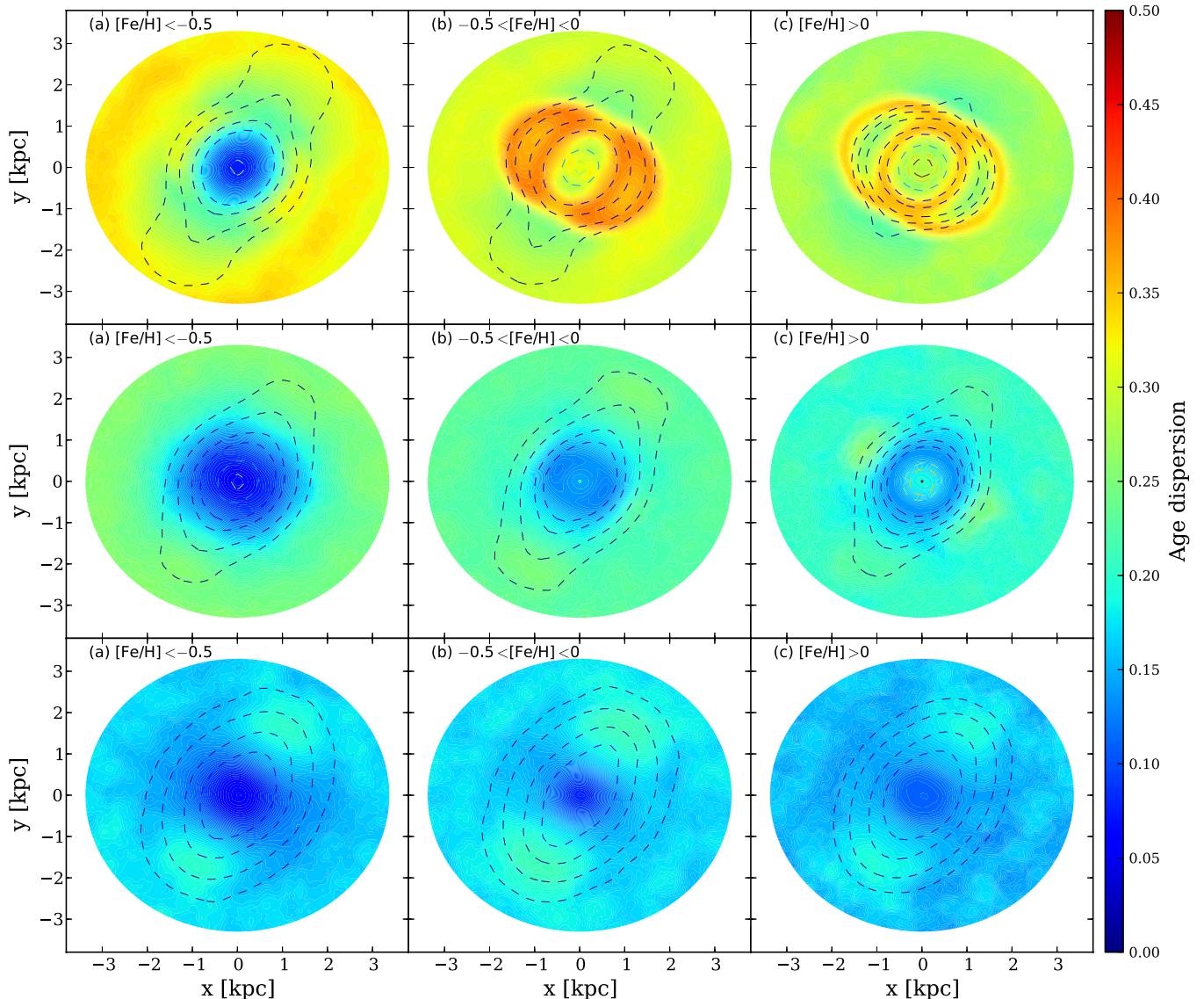


Figure 4. Age dispersion of stars in the inner $R < 3$ kpc of the simulation with the same slices in $|z|$ and $[\text{Fe}/\text{H}]$ bins as Figure 3. (A color version of this figure is available in the online journal.)

higher latitudes in the bulge, and that there is a broader range of ages for the metal-rich stars whereas the metal-poor stars are predominantly old. Our comparison of the stellar ages in the model to the microlensed dwarfs is informed by the middle and bottom panels of Figures 3 and 4. The top panels show that the trend of old stars at low $[\text{Fe}/\text{H}]$ and a range of ages at high $[\text{Fe}/\text{H}]$ continues to the plane, with decreasing ages moving closer to the plane for the metal-rich stars, and old stars even in the plane for the metal-poor stars.

This distribution of stars including the youngest population in the plane, driven by the evolution of the bar, is similar to the star formation regions seen in barred disk galaxies in general (Kormendy & Kennicutt 2004).

The old population at the very center of the model formed early from a thick disk and the younger stars are from ongoing star formation in the plane associated with the dynamical formation processes. This recent star formation happens naturally without any tuning. The star formation history is partly driven by the gas inflow to the center and related to how strong the bar is at any particular time.

According to these figures, a median old stellar population is expected to be observed for most fields in the bulge, located even a few degrees from the plane. Although a somewhat younger mean population of stars is present at the ends of the bar, including at $3^\circ < |b| < 6^\circ$, it is difficult to isolate this population observationally for stars integrated along a given line of sight. Only photometric observations that target the near end of the bar close to the plane ($l \sim 12^\circ$, $|b| < 3^\circ$) should reveal a slightly younger mean population compared to the inner longitudes. The photometric studies that report old isochrones as the best-fit models to fields at $(l, b) = (+1^\circ, -2^\circ 9')$ (Ortolani et al. 1995), $(+0^\circ 3, -6^\circ 2')$ (Zoccali et al. 2003), $(+1^\circ 25, -2^\circ 65')$ (Sahu et al. 2006), and $(+10^\circ 3, -4^\circ 2')$, $(-6^\circ 8, 4^\circ 7')$ (Valenti et al. 2013) are consistent with the predictions of this model.

4.2. The Age Distribution of Stars Across $[\text{Fe}/\text{H}]$

To study the age distribution as a function of metallicity in the model, we now examine the three metallicity ranges as shown in Figures 3(a)–(c) and 4(a)–(c), individually. There is clearly

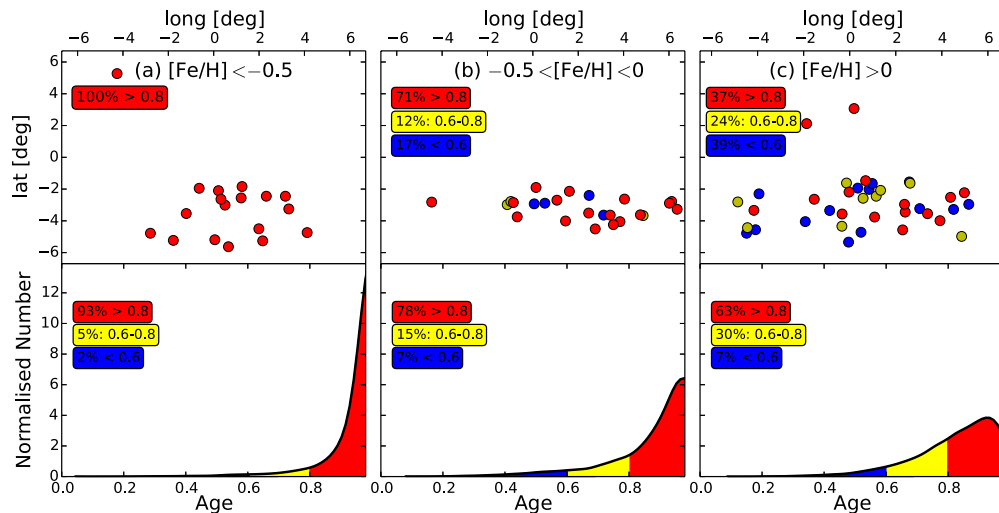


Figure 5. Top panels show the location on the sky of the 80 microlensed bulge dwarfs with the metallicity intervals (a)–(c) as indicated on the top of each panel. The colors represent ages $> 80\%$ of the maximum age (red), $60\% < \text{ages} < 80\%$ (yellow), and ages $< 60\%$ of the oldest stars. The bottom panels show the total normalized age distribution of targets selected at these (l, b) positions in the simulation. The percentage of stars in each age bin are shown in each sub-panel.

(A color version of this figure is available in the online journal.)

a different age distribution for the most metal-rich versus the most metal-poor stars.

The model shows that at a given height from the plane, the more metal-rich stars will be, *on average*, younger than the more metal-poor stars and that there is an age gradient with distance from the plane for the metal-rich stars. The age gradient is *shallower* at larger heights and the age distribution becomes increasingly older and has a smaller age dispersion farther away from the plane. For the metal-rich stars in sub-panels (b) and (c), with $[\text{Fe}/\text{H}] > -0.5$, the predominantly younger stars are concentrated to the plane and extend to the innermost bulge at the highest metallicities. There is also a wide dispersion in age nearest to the plane, where both young and old stars will be observed.

The young population we refer to when we compare to the microlensing results is seen in the regions of the observations in the middle and bottom panels of Figures 3 and 4. The age distribution of the metal-rich stars extends from ages $< 50\%$ to $> 90\%$ of the oldest stars in the simulation. For the metal-poor stars, $[\text{Fe}/\text{H}] < -0.5$, the model ages are on the order of 80% – 100% of the maximum ages. We stress that these are not very young (< 1 Gyr) stars.

For the metal-poor stars, $[\text{Fe}/\text{H}] < -0.5$, shown in panel (a), the model predicts that an old population is expected in the bulge, with younger stars located near the ends of the bar. Old stars of comparable ages to the bulge stars are also located in the nearby surrounding disk. This is an important prediction of the model: a metal-rich star within $|b| < 6^\circ$ from the plane in the bulge and the nearby surrounding disk can have a range of ages, with preferentially younger stars at the highest metallicities and lower latitudes, but a metal-poor star in the bulge, regardless of latitude, will almost always be old. Observationally, the metallicity limit between these regimes in the Milky Way appears around $[\text{Fe}/\text{H}] \approx -0.4$ (see Figure 1). The top panels of Figure 5 show the (l, b) of the microlensed dwarf sample, as a function of metallicity and color coded by age, normalized to a maximum age of 13.6 Gyr. The bottom panels of Figure 5 show the corresponding age distribution for stars at these locations in the simulation normalized to an age of 10 Gyr. Figure 5 shows that although the number of youngest stars in the microlensed dwarf sample are not reproduced, with far fewer stars at the

youngest ages in the model compared to the data, the observed metal-poor stars are all old and present at low and high latitudes and the dispersion in the ages of the stars increases as a function of $[\text{Fe}/\text{H}]$, in agreement with the distribution seen in the model. From comparing the age distribution for all stars as a function of metallicity, it is clear that studies of individual stars are necessary to test the range of ages of stars in the inner Galaxy.

5. CONCLUSION

Multiple channels of evidence including the kinematics (Kunder et al. 2012; Shen et al. 2010; Ness et al. 2013a), the X-shaped morphology (McWilliam & Zoccali 2010; Nataf et al. 2010; Ness et al. 2012; Li & Shen 2012), and now ages, as we have demonstrated in this Letter, indicate that the bulge of the Milky Way is in large part, if not entirely, formed as part of the evolution of the disk. This is at odds with the merger formation scenario predicted by early semi-analytic models and a significant problem for the assumption that the bulge must have been accreted (Guo et al. 2011; Zavala et al. 2012; Cooper et al. 2013), given that Milky Way type galaxies are common in the universe. Our results demonstrate that merger processes are not necessary to form the old bulge population that has been previously associated with a classical bulge in simulations (Doménech-Moral et al. 2012; Obreja et al. 2013) and early bulge-forming dissipational collapse in the Milky Way (Zoccali et al. 2003; Babusiaux et al. 2010; Hill et al. 2011). This result is important as it demonstrates that old stars are not unique to a classical bulge and younger stars that are distributed nearer to the plane and metal-rich stars spanning a range of ages are a signature of a bulge formed via internal evolution processes. Our analysis is qualitative and our simulation is not designed to match the Milky Way and is suitable for a generalized comparison to disk galaxies. Observations of other disk galaxies have also shown that photometry and spectroscopy can reveal different results for stellar ages (e.g., MacArthur et al. 2009) and the generic signatures in the stellar ages we report in this Letter inform the overall picture in the internal evolution of disk galaxies (e.g., Kormendy & Kennicutt 2004; Sellwood 2014). Our results do not exclude any contribution of a merger event but simply demonstrate that old stars need not exclude a purely

internal origin and younger stars in an otherwise old bulge are a natural outcome of internal evolution in the Milky Way. Our results are in agreement with the bulge formation as a dynamical process from the disk at early times reported by Guedes et al. (2013) whereby the majority of stars are old. In our analysis, we show that the presence of the young stars near the plane in the simulations is an important aspect of bulge formation via disk evolution, and one that matches well the observations (Bensby et al. 2013). Thus the observed ages of stars within the Milky Way bulge can be explained within the context of internal formation and dynamical processes, consistent with other lines of evidence supporting a bulge largely forming from the disk. The key question we now endeavor to resolve, with respect to the Milky Way bulge as a signature of the Galaxy's formation, is what fraction of stars, if any, are part of a merger remnant? Mapping the age distribution of the bulge as a function of l and b and performing further quantitative analyses that our team is preparing, examining key regions highlighted in this Letter, and further comparisons to models in the spirit of this Letter, are critical to interpret observations and understand the formation of the Milky Way.

The research has received funding from the European Research Council under the European Union's Seventh Framework Programme (FP 7) ERC Grant Agreement No. [321035]. T.B. was funded by grant No. 621-2009-3911 from The Swedish Research Council. V.P.D. and D.R.C. are supported by STFC Consolidated grant # ST/J001341/1. The simulation used in this Letter was run at the High Performance Computing Facility of the University of Central Lancashire. We thank Laurent Serge Noel of the University of Central Lancashire for Figure 2. We thank the GREAT ESF program for funding that has supported this research.

REFERENCES

- Babusiaux, C., Gómez, A., Hill, V., et al. 2010, *A&A*, **519**, A77
 Barentine, J. C., & Kormendy, J. 2012, *ApJ*, **754**, 140
 Bensby, T., Adén, D., Meléndez, J., et al. 2011, *A&A*, **533**, A134
 Bensby, T., Yee, J. C., Feltzing, S., et al. 2013, *A&A*, **549**, A147
 Brown, T. M., Sahu, K., Anderson, J., et al. 2010, *ApJL*, **725**, L19
 Clarkson, W., Sahu, K., Anderson, J., et al. 2008, *ApJ*, **684**, 1110
 Combes, F., & Sanders, R. H. 1981, *A&A*, **96**, 164
 Cooper, A. P., D'Souza, R., Kauffmann, G., et al. 2013, *MNRAS*, **434**, 3348
 Doménech-Moral, M., Martínez-Serrano, F. J., Domínguez-Tenreiro, R., & Serna, A. 2012, *MNRAS*, **421**, 2510
 Gardner, E., Debattista, V. P., Robin, A. C., Vásquez, S., & Zoccali, M. 2014, *MNRAS*, **438**, 3275
 Gilmore, G., Wyse, R. F. G., & Jones, J. B. 1995, *AJ*, **109**, 1095
 Guedes, J., Mayer, L., Carollo, M., & Madau, P. 2013, *ApJ*, **772**, 36
 Guo, Q., White, S., Boylan-Kolchin, M., et al. 2011, *MNRAS*, **413**, 101
 Hill, V., Lecureur, A., Gómez, A., et al. 2011, *A&A*, **534**, A80
 Howard, C. D., Rich, R. M., Reitzel, D. B., et al. 2008, *ApJ*, **688**, 1060
 Kormendy, J., & Kennicutt, R. C. 2004, *ARA&A*, **42**, 603
 Kunder, A., Koch, A., Rich, R. M., et al. 2012, *AJ*, **143**, 57
 Li, Z.-Y., & Shen, J. 2012, *ApJL*, **757**, L7
 López-Corredoira, M., Cabrera-Lavers, A., & Gerhard, O. E. 2005, *A&A*, **439**, 107
 Lütticke, R., Pohlen, M., & Dettmar, R.-J. 2004, *A&A*, **417**, 527
 MacArthur, L. A., González, J. J., & Courteau, S. 2009, *MNRAS*, **395**, 28
 McWilliam, A., & Zoccali, M. 2010, *ApJ*, **724**, 1491
 Nataf, D. M., Udalski, A., Gould, A., Fouqué, P., & Stanek, K. Z. 2010, *ApJL*, **721**, L28
 Navarro, J. F., Frenk, C. S., & White, S. D. M. 1997, *ApJ*, **490**, 493
 Ness, M., Freeman, K., Athanassoula, E., et al. 2012, *ApJ*, **756**, 22
 Ness, M., Freeman, K., Athanassoula, E., et al. 2013a, *MNRAS*, **430**, 836
 Ness, M., Freeman, K., Athanassoula, E., et al. 2013b, *MNRAS*, **432**, 2092
 Obreja, A., Domínguez-Tenreiro, R., Brook, C., et al. 2013, *ApJ*, **763**, 26
 Ortolani, S., Renzini, A., Gilmozzi, R., et al. 1995, *Natur*, **377**, 701
 Raha, N., Sellwood, J. A., James, R. A., & Kahn, F. D. 1991, *Natur*, **352**, 411
 Robin, A. C., Luri, X., Reylé, C., et al. 2012, *A&A*, **543**, A100
 Roškar, R., Debattista, V. P., Stinson, G. S., et al. 2008, *ApJL*, **675**, L65
 Sahu, K. C., Casertano, S., Bond, H. E., et al. 2006, *Natur*, **443**, 534
 Sellwood, J. A. 2014, *RvMP*, **86**, 1
 Shen, J., Rich, R. M., Kormendy, J., et al. 2010, *ApJL*, **720**, L72
 Valenti, E., Zoccali, M., Renzini, A., et al. 2013, *A&A*, **559**, 98
 Wegg, C., & Gerhard, O. 2013, *MNRAS*, **435**, 1874
 Zavala, J., Avila-Reese, V., Firmani, C., & Boylan-Kolchin, M. 2012, *MNRAS*, **427**, 1503
 Zoccali, M., Renzini, A., Ortolani, S., et al. 2003, *A&A*, **399**, 931